Locally Periodic Kernel-Based Regression to Identify Time-Varying Ankle Impedance during Locomotion

A Simulation Study

Cavallo, Gaia; Schouten, Alfred C.; Lataire, John

DOI
10.1109/EMBC44109.2020.9175835

Publication date
2020

Document Version
Final published version

Published in
Proceedings of the 42nd Annual International Conferences of the IEEE Engineering in Medicine and Biology Society, EMBC 2020

Locally Periodic Kernel-Based Regression to Identify Time-Varying Ankle Impedance During Locomotion: a Simulation Study*

Gaia Cavallo, *Student member, IEEE*, Alfred C. Schouten, and John Lataire, *Member, IEEE*

Abstract— Human joint impedance is a fundamental property of the neuromuscular system and describes the mechanical behavior of a joint. The identification of the lower limbs' joints impedance during locomotion is a key element to improve the design and control of active prostheses, orthoses, and exoskeletons. Joint impedance changes during locomotion and can be described by a linear time-varying (LTV) model. Several system identification techniques have been developed to retrieve LTV joint impedance, but these methods often require joint impedance to be consistent over multiple gait cycles. Given the inherent variability of neuromuscular control actions, this requirement is not realistic for the identification of human data. Here we propose the kernel-based regression (KBR) method with a locally periodic kernel for the identification of LTV ankle joint impedance. The proposed method considers joint impedance to be periodic yet allows for variability over the gait cycles. The method is evaluated on a simulation of joint impedance during locomotion. The simulation lasts for 10 gait cycles of 1.4 s each and has an output SNR of 15 dB. Two conditions were simulated: one in which the profile of joint impedance is periodic, and one in which the amplitude and the shape of the profile slightly vary over the periods. A Monte Carlo analysis is performed and, for both conditions, the proposed method can reconstruct the noiseless simulation output signal and the profiles of the time-varying joint impedance parameters with high accuracy (mean VAF ~ 99.9% and mean normalized RMSE of the parameters 1.33-4.06%).

The proposed KBR method with a locally periodic kernel allows for the identification of periodic time-varying joint impedance with cycle-to-cycle variability.

I. Introduction

To improve the design and control of active prostheses, orthoses, and exoskeletons, the need for a model of the lower limbs' mechanical properties during locomotion is advocated in the literature [1,2,3]. Having an accurate model of lower limbs' joint impedance during locomotion is a key element to render the assistive devices more natural and versatile. Commonly, human joint impedance is used to provide an intuitive description of the mechanical behavior of a joint. Joint impedance is a fundamental property of the neuromuscular system [1] and is defined as the dynamic relationship between the angular deviation of a human joint and the resulting torque acting about it [4]. In other words, joint impedance describes how much a joint resists angular perturbations. During movements, the human joint impedance varies depending on factors such as the joint angle and the muscular activation level. Therefore, under a modeling perspective, joint impedance during locomotion can be described by a linear time-varying (LTV) system.

Accurate LTV modeling of the human joint impedance during locomotion remains a challenge, partially due to the inherent variability and complexity of the neuromuscular control actions. A first attempt of identification during locomotion was performed by [1], where ankle impedance was identified from the pre-swing phase to the early-loading response using an LTV ensemble technique and from the late-loading response to terminal stance using multiple LTI estimations. The devices used were, respectively, an orthotic device capable of applying small-amplitude perturbations to the joint, and a platform which applies ramp perturbations at specific phases of the gait cycle. In these approaches, joint impedance was described with an inertia-spring-damper model. The results provide a valuable indication of how joint damping and stiffness of the ankle vary during the gait cycle.

In addition, several studies have been carried out in which joint impedance identification was tested in simulation or in simplified experimental conditions where the joint of interest was perturbed while the subjects maintained a stationary position. A valuable example is given in [5], where a complex hybrid LTV estimation technique was developed to identify the intrinsic and reflexive properties of the ankle impedance, giving a full picture of the neuromuscular processes affecting the mechanical properties of the joint. The method is currently applied for human joint impedance identification during experimental conditions where the periodicity of the human behavior is assumed to repeatable. However, given the inherent variability of neuromuscular control actions, during periodic actions such as locomotion, the periodicity of the joint impedance over the gait cycle is subject to variations.

In this article, an LTV method is proposed which exploits the periodicity of the joint impedance yet does not require an exact repeatability of the joint impedance over periods.
The joint impedance is represented by an inertia-spring-damper model, where the inertia, damping, and stiffness are retrieved using a Bayesian probabilistic approach, named the kernel-based regression (KBR) method.

The KBR method has been previously applied to the identification of joint impedance in [6]. In the current study,

* This work was financially supported by the Research Foundation Flanders (FWO-Vlaanderen, PhD fellowship nr 1182019N), and by the Flemish Government (Methusalem Fund METH1).

G. Cavallo and J. Lataire are with the Department ELEC, Vrije Universiteit Brussel, Pleinlaan 2, 1050, Brussels, Belgium. (corresponding author e-mail: gaia.cavallo@vub.be).

A. C. Schouten is with the Biomechanical Engineering Department, TU Delft, Mekelweg 2, 2628 CD, Delft, The Netherlands.

978-1-7281-1990-8/20/$31.00 ©2020 IEEE

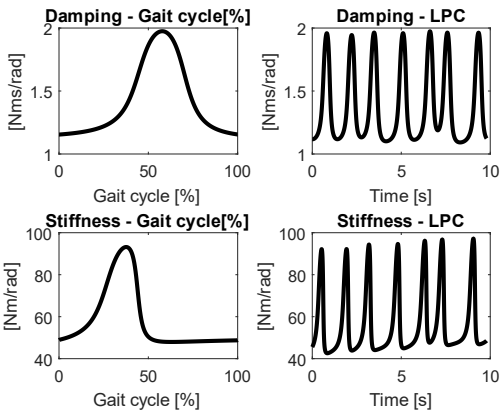

Figure 1. First column: Profile used in the simulation of the damping (first row) and stiffness (second row) in function of the percentage of the gait cycle. Second column: Example of a profile of the damping (first row) and stiffness (second row) used in the simulation for the locally periodic condition. The profiles are in function of time.

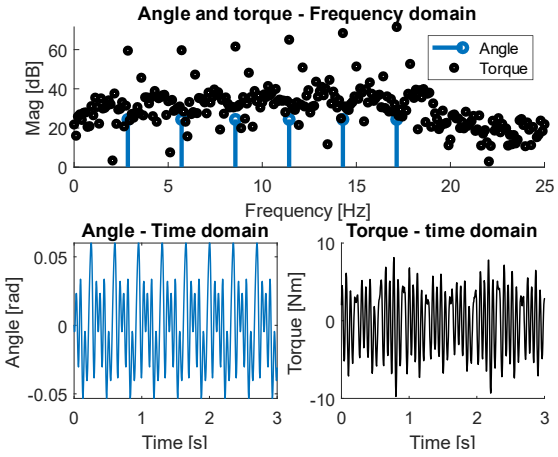

Figure 2. Input angular position and simulated output torque signals after preprocessing for one realization obtained using the locally periodic condition. The first row represents the signals in the frequency domain and the second row the signals in the time domain.

the method is modified to be applicable to ankle joint impedance identification during (quasi)periodic data, like locomotion. Under a Bayesian probabilistic perspective, we express that the damping and the stiffness parameters are likely to be approximately periodic. The KBR method, briefly described in Section II.B, is applied to the identification of a simulation model representative of ankle impedance during locomotion.

II. Method

A. Simulation

A simulation is performed in which the dynamics of the ankle joint are represented by a second-order inertia-spring-damper model. The equation used to represent the system is given by:

$$\tau(t) = I\frac{d^2(\phi(t))}{dt^2} + B(t)\frac{d(\phi(t))}{dt} + K(t)\phi(t) + n(t) \quad (1)$$

Where $\tau(t)$ is the simulated output torque, $\phi(t)$ is the input angular position, $n(t)$ is the additive zero-mean Gaussian noise, I is the inertia, $B(t)$ and $K(t)$ are the time-varying damping and stiffness. The profiles for the damping and stiffness during one gait cycle, shown in the first column of Fig.1, are representative of the values during locomotion and are based on [1,7]. The simulated inertia, representing the time-invariant inertia of the foot, is set to 0.02 Nms^2/rad.

The model is simulated for 14 s and is composed of the repetition of 10 gait cycles of 1.4 s each. The length of the gait cycle is chosen to represent slow-walking [8]. The input of the system is a random phase multisine, with root-mean-square amplitude 0.03 rad and a period of length 0.35 s. This corresponds to 4 repeated periods of the multisine for each gait cycle. The maximum excitation frequency is ~17 Hz. Zero-mean Gaussian noise is added to the torque, resulting in a signal-to-noise ratio of around 15 dB. The sampling frequency is 2000 Hz. Two conditions for the damping and stiffness are chosen:

i) Periodic condition (PC): The damping and the stiffness are periodic and the profile for one gait cycle is repeated at every gait cycle. This condition provides a framework to test the accuracy of the estimation method.

ii) Locally periodic condition (LPC), Fig. 1: A cycle-to-cycle variability of the damping and stiffness profiles is introduced. The shape of the profiles is roughly the same for every gait cycle, although there is variability in the vertical and horizontal position of the peak values. The variability is random for every gait cycle and each peak can have a maximum deviation of 4% from the nominal value. This condition is more realistic for human experiments, where variability is expected, and it provides a framework to check the robustness of the identification method.

For both the periodic and the locally periodic conditions, 100 input/output realizations are obtained in simulation, creating a dataset for Monte Carlo analysis. The data is then preprocessed: the first 4.2 s are removed from the input/output to avoid the transient effects, the data is resampled to 200 Hz and converted to the frequency domain. Only the bins in the frequency band between 0 and 25 Hz are used for the identification. An example of the data after preprocessing is given in Fig. 2.

B. Identification method

A second-order differential equation is used to model the system (1). The model parameters are the damping and stiffness, represented by smooth functions of time, and the constant (i.e. time-invariant) inertia. The model parameters are retrieved using the KBR method. The approach is intuitively explained below, following the interpretation given in [9], while an extensive and analytical description can be found in [10].

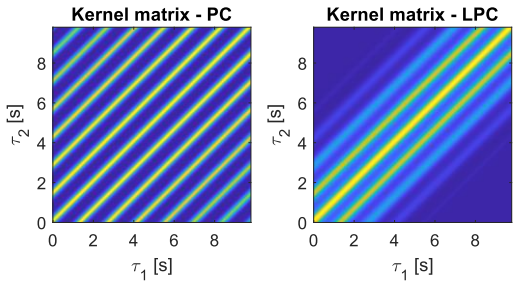

Figure 3. Kernel matrices used for the periodic (left) and locally periodic (right) condition, representing the covariance between the time-varying parameter at time τ_1 and at time τ_2. The matrices are composed of an array of scalars ranging from 0 (dark blue) to 1 (yellow).

In traditional LTV regression methods the model parameters are described by a fixed set of basis functions, whilst in KBR the model parameters are described by a family of functions associated with the same covariance matrix. The covariance matrix, named the kernel matrix, depends on a set of hyperparameters that strongly affect the properties of the model parameters. Different kernels with different hyperparameters can be constructed depending on the expected time-varying behavior of the underlying system. Typical hyperparameters are smoothness and output variance. In this study, the periodicity is an additional hyperparameter since we analyze a (quasi)periodic time-varying systems. A locally periodic kernel is used, and the related kernel matrix is represented in Fig. 3 for the periodic (left column) and locally periodic (right column) conditions. The hyperparameters used for the periodic and locally periodic conditions can be extracted from the kernel matrix in Fig. 3 as follows:

Periodicity length. The length of the periodicity corresponds to the distance between the yellow antidiagonal lines. For both conditions, the periodicity length is set to 1.4 s, which is the length of the gait cycle.

Periodicity consistency: The consistency of the periodicity is inversely proportional to the speed at which the covariance decreases over time. In the periodic condition, the periodicity is consistent, therefore the covariance is very close to 1 at periodic intervals, resulting in multiple yellow lines. In the locally periodic condition, the periodicity is more variable, resulting in a decay of the covariance over periods.

Smoothness of the time variation: The width of the main antidiagonal line is inversely proportional to the smoothness of the time variation. The parameter is roughly the same for the periodic and locally periodic conditions.

Output variance: The output variance, which is not directly observable from Fig. 3, is selected according to the SNR of the output after resampling.

C. Performance indicators

For each realization, the estimates of the inertia, damping, and stiffness parameters are computed using the KBR approach. The accuracy of the estimated parameters is expressed in terms of the average normalized root-mean-square error ($\overline{RMSE}$) between the estimated and the simulated parameters. The formula is expressed in (2), where $P = B, K$ and the denominator serves as a normalization factor:

$$\overline{RMSE} = \sqrt{\frac{\left(\sum_{k=1}^{N_{mc}} \sum_{i=1}^{N} \left(P_k(t_i) - \hat{P}_k(t_i)\right)^2\right)}{\sum_{k=1}^{N_{mc}} \sum_{i=1}^{N} \left(P_k(t_i)\right)^2}} \cdot 100\% \qquad (2)$$

Where N_{mc} is the number of Monte Carlo realizations, N the number of data points in each realization, $P_k(t_i)$ and $\hat{P}_k(t_i)$ represent, respectively, the simulated and the estimated values of the damping and stiffness at time t_i, for the Monte Carlo realization k. The average normalized root-mean-square standard deviation ($\overline{SD}$) and bias ($\overline{Bias}$) are computed as well in the same fashion and are such that $\overline{RMSE}^2 = \overline{SD}^2 + \overline{Bias}^2$. Moreover, the variance-accounted-for (VAF_k) between the simulated noiseless torque and the estimated torque is computed as:

$$VAF_k = \left(1 - \frac{var(\tau_k(t) - \hat{\tau}_k(t))}{var(\tau_k(t))}\right) \cdot 100\% \qquad (3)$$

Where τ_k and $\hat{\tau}_k$ are the simulated and estimated torque for the realization k, and var the variance operation. The average over the Monte Carlo realizations is computed, giving the $\overline{VAF}$.

III. Results

TABLE I. Monte Carlo accuracy for the periodic and locally periodic conditions.

Monte Carlo Accuracy	*Damping*			*Stiffness*			*Torque*
	$\overline{RMSE}$ [%]	$\overline{SD}$ [%]	$\overline{Bias}$ [%]	$\overline{RMSE}$ [%]	$\overline{SD}$ [%]	$\overline{Bias}$ [%]	$\overline{VAF}$ [%]
PC	1.33	0.69	1.15	2.53	1.86	1.61	99.98
LPC	2.36	1.42	1.90	4.15	3.13	2.74	99.96

The simulated damping and stiffness profiles and their estimates for the periodic condition are plotted in the first column of Fig. 4. The dotted black line represents the simulated value of the profiles, the orange line the mean of the estimates over the Monte Carlo realizations and the green area the standard deviation. The accuracy of the estimation is shown in Table I. The estimates track the simulated profiles with small errors ($\overline{RMSE}$ of 1.33% for the damping and 2.53% for the stiffness) and the mean of the estimate is close to the simulated value, with a $\overline{Bias}$ of 1.15% for the damping and 1.61% for the stiffness. The consistency of the estimator is high, and the standard deviation area is barely visible. The corresponding $\overline{SD}$ is 0.69% for the damping and 1.61% for the stiffness. In the first row of Fig. 5, the simulated noiseless torque from a single realization is plotted versus the estimated torque. The fit between the two signals is very close. The $\overline{VAF}$ is 99.98%.

The second column of Fig. 4 represents the damping and stiffness estimate for the locally periodic condition. Since, in this case, the simulated profiles changed at every realization, the plot is given for a single realization. The estimates closely track the simulated value, with some small deviation,

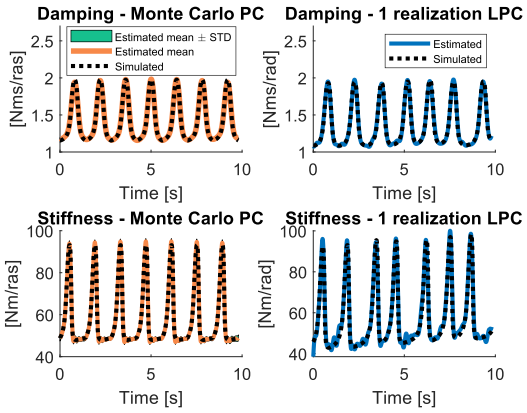

Figure 4. Simulated (dotted line) and estimated (continuous line) damping (first row) and stiffness (second row). For the periodic condition (first column), the estimate is shown for 100 realizations, and the mean (orange) and the mean ± standard deviation (green area) are represented. For the locally periodic condition, the estimate is shown for one realization (blue line).

especially in the low amplitude areas. The $\overline{RMSE}$ of the damping and the stiffness, of respectively 2.36% and 4.15%, are higher than for the periodic condition. The $\overline{SD}$ are higher as well (1,.42% and 3.13%), while the $\overline{VAF}$ is comparable. The estimate of the inertia is not shown since it is equal to the simulated value for all the realizations.

IV. Discussion

Even though in the KBR a fairly open structure for the time variation is used, the method could reconstruct the time-varying damping and stiffness profiles with high accuracy in both of the tested conditions. This can be confirmed in Fig. 4, where a close tracking of the simulated profiles can be observed.

As expected, the $\overline{RMSE}$ for the locally periodic condition is higher than for the periodic one. A cause for this increased error is the presence of oscillations of the estimate around the simulated value, especially evident for the stiffness profile in the areas of low amplitude. The oscillations explain the increased $\overline{SD}$. There is a bias of the estimate, which affects the accuracy as well. It can be concluded that the estimate of the profiles tracks the simulated value, although there is some small error, mainly because the estimate is less smooth than the simulated value. The small errors in the parameters had little effects on the estimation of the system output and the estimator is robust with respect to the variability of the periodic profiles.

In the current simulation, the inertia is time-invariant, and the length of the gait cycle is constant over periods. However, the presented KBR method can deal as well with time-varying inertia and a variable period length. Given the realistic simulation conditions, with low SNR, short measurement time and human-like time-varying damping and stiffness profiles, the presented method has good potentials to be applied to actual measurements from humans.

A limitation of the presented study is that it does not consider the reflexive properties of the joint impedance.

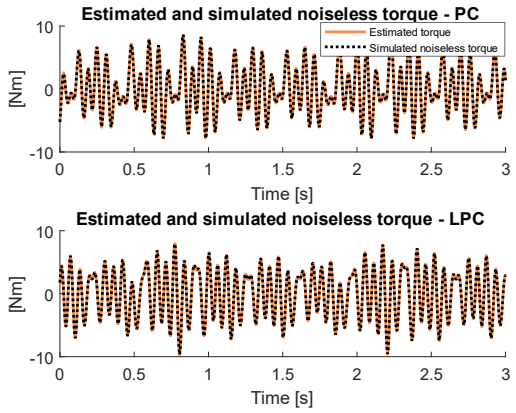

Figure 5. Estimated torque (orange) and simulated noiseless torque (dotted black line) for the periodic condition (first row) and the locally periodic condition (second row) on a single realization.

V. Conclusions

The study presents a proof of concept of the applicability of the KBR method with a locally periodic kernel to the identification of human-like intrinsic ankle impedance with cycle-to-cycle variability. The method shows promising results and additional work is being done to apply the method to real human experimental data, where the actual torque and angle profiles of the ankle joint during locomotion are reproduced.

References

[1] H. Lee, E. J. Rouse, and H. I. G. O. Krebs, "Summary of Human Ankle Mechanical Impedance During Walking," IEEE J. Transl. Eng. Heal. Med., vol. 4, no. August, 2016.

[2] E. Perreault, L. J. Hargrove, D. Ludvig, H. Lee, and J. Sensinger, "Considering Limb Impedance in the Design and Control of Prosthetic Devices," in Neuro-Robotics: From Brain Machine Interfaces to Rehabilitation Robotics, vol. 2, Springer, 2014, pp. 59–83.

[3] K. Shamaei, G. S. Sawicki, and A. M. Dollar, "Estimation of Quasi-Stiffness of the Human Knee in the Stance Phase of Walking," vol. 8, no. 3, 2013.

[4] N. Hogan, "Adaptive Control of Mechanical Impedance by Coactivation of Antagonist Muscles," IEEE Trans. Automat. Contr., vol. 29, no. 8, pp. 681–690, 1984.

[5] D. L. Guarin and R. E. Kearney, "Unbiased Estimation of Human Joint Intrinsic Mechanical Properties during Movement," IEEE Trans. Neural Syst. Rehabil. Eng., vol. 26, no. 10, pp. 1975–1984, 2018.

[6] M. Van De Ruit, G. Cavallo, et al., "Revealing Time-Varying Joint Impedance With Kernel-Based Regression and Nonparametric Decomposition," IEEE Trans. Control Syst. Technol., vol. PP, pp. 1–14, 2018.

[7] D. L. Guarín and R. E. Kearney, "Estimation of Time-Varying, Intrinsic and Reflex Dynamic Joint Stiffness during Movement. Application to the Ankle Joint," *Front. Comput. Neurosci.*, vol. 11, no. June, pp. 1–17, 2017.

[8] T. Sinkjær, J. B. Andersen, & B. I. R. G. I. T. Larsen, "Soleus stretch reflex modulation during gait in humans," Journal of neurophysiology, vol. 76, no. 2, pp 1112-1120, 1996

[9] C. E. Rasmussen and C. K. I. Williams. "Gaussian Processes for Machine Learning. " MIT Press, 2006.

[10] J. Lataire, R. Pintelon, D. Piga, and R. Tóth, "Continuous-time linear time-varying system identification with a frequency-domain kernel-based estimator," IET Control Theory Appl., vol. 11, no. 4, pp. 457–465, 2017.